JOURNAL OF SOLID STATE CHEMISTRY 28, 329–343 (1979)

The Ligand-Field Spectrum of Fe^{3+} in Garnets

P. KÖHLER* AND G. AMTHAUER†

** Fachbereich Chemie and † Institut für Mineralogie der Philipps-Universität Marburg, Lahnberge, 3550 Marburg, Federal Republic of Germany*

Received May 10, 1978; in final form August 24, 1978

The ligand-field spectra of garnets bearing Fe^{3+} exclusively at the octahedral as well as at the octahedral and tetrahedral sites have been studied at energies between 8000 and 30 000 cm^{-1}. The absorption bands up to 28 000 cm^{-1} have been assigned by comparison of experimental and calculated transition energies obtained by a complete solution of the d^5 energy matrices. The Racah parameters of Fe^{3+} in both positions have been reinterpreted using a constant C/B ratio evaluated from the gaseous Fe^{3+} ion. It was found that the octahedral B parameters are always larger than the tetrahedral ones. The results are consistent with isomer shifts of ^{57}Fe and the observed structural features in oxide garnets.

Introduction

During the past few years, the problem of the cation distribution in crystal structures of chemically complex garnets has been studied in considerable detail. The analysis of the Mössbauer spectrum of ^{57}Fe in garnets (*1–5*) has permitted an unambiguous, precise determination of the occupancies of ferric and ferrous iron at the eight-, six-, and four-fold coordinated sites. The ligand-field spectra of natural and synthetic garnets have also been studied independently (*6–12*). Here, however, different assignments of the absorption bands of Fe^{3+} in the tetrahedral and octahedral sites in the range 20 700 to 27 000 cm^{-1} are reported (Table I). In the case of silicate garnets, for example, Moore and White (*9*) assigned the absorption band at 21 758 cm^{-1} in grossular $Ca_3(Al, Fe^{3+})_2Si_3O_{12}$ (sample Gr-74) to the transition $^6A_1 \rightarrow {}^4A_1, {}^4_bE$ of tetrahedral Fe^{3+}, whereas Manning (*8*) assigned the band at 23 900 and 24 400 cm^{-1} to that transition in andradite $Ca_3Fe^{3+}Si_3O_{12}$. On the other hand, the maximum at 24 500 cm^{-1} in yttrium iron garnet (YIG) was interpreted by Vien *et al.* (*12*) as the transition to the ^4E_g level of octahedral Fe^{3+}. Moore and White (*9*) reported this transition to be at 27 040 cm^{-1} in grossular (sample Gr-74). While the energies of these levels are expected to be Δ-independent (cf. Table IVa, b), such apparent shifts would imply a wide range of the interelectronic repulsion parameter in the garnet structure. Hence values of 650 cm^{-1} (*12*) and 800 cm^{-1} (*10*), respectively, are reported for B(tet), while the given B(oct) values vary between 460 cm^{-1} (*12*) and 700 cm^{-1} (*10*). Surprisingly, B(oct) is always found to be smaller than B(tet) (cf. Table I) from these references, indicating an apparently less covalent Fe–O bond in the tetrahedron compared to that of the octahedron. The ligand-field parameter Δ(oct) is calculated between 12 000 and 13 000 cm^{-1}, whereas Δ(tet) varies between 5550 and 6700 cm^{-1} (cf. Table I).

In this paper a consistent reinterpretation of the ligand-field spectra of Fe^{3+} in garnets is presented, based on our own

0022-4596/79/060329-15$02.00/0

TABLE I

LIGAND-FIELD PARAMETERS AND OBSERVED ABSORPTION BANDS BETWEEN 20 000 AND 28 000 cm^{-1} AND THEIR ASSIGNMENTS (REVIEW)[a]

Compound	Energy level (cm^{-1})						B(o) (cm^{-1})	B(t) (cm^{-1})	Δ(o) (cm^{-1})	Δ(t) (cm^{-1})	Ref.
	$^4A_1, {}^4_aE(t)^b$	$^4A_{1g}, {}^4_aE_g(o)^b$	$^4_bT_2(t)^b$	$^4_bT_{2g}(o)^b$	$^4_bE(t)^b$	$^4_bE_g(o)^b$					
$Y_3Fe_5O_{12}$	20 800	21 150	23 300	22 600	25 700	24 100	460	650	12 700	6700	(*12*)
$Y_3Fe_5O_{12}$	20 710	21 390	24 150	22 520	—	—	530	705	13 000	5600	(*11*)
$Y_3(Al, Fe)_5O_{12}$	21 190	20 530	24 210	22 940	27 320	24 450	700	800	12 700	6200	(*10*)
$Ca_3Fe_2Si_3O_{12}$[c]	—	22 701 22 999	—	24 000	—	—	614	614	12 600	5550	(*9*)
$Ca_3(Al, Fe)_2(Si, Fe)_3O_{12}$[d]	21 758	22 865 23 121	—	23 952	26 400	27 040	614	614	12 600	5550	(*9*)
$Ca_3Fe_2Si_3O_{12}$[c]	23 900 24 400	22 700	—	—	—	26 000	—	—	—	—	(*8*)
$Ca_3(Al, Fe)_2Si_3O_{12}$[d]	—	23 100	—	—	—	27 000	557	—	—	—	(*7*)
$Ca_3Fe_2Si_3O_{12}$[c]	—	22 850	—	—	—	27 000	593	—	—	—	(*7*)

[a] The four absorption bands between 11 000 and 20 000 cm^{-1} are interpreted by most of the authors as the transitions to the levels $^4_aT_{1g}$, $^4_aT_{2g}$, $^4_aT_1$, and $^4_aT_2$.

[b] (t) = tetrahedral. (o) = octahedral.

[c] Natural garnet andradite.

[d] Natural garnet grossular.

measurements of the absorption spectra of nine oxide garnets with known cation distributions obtained from Mössbauer spectra. It will be shown that all absorption bands between 10 000 and 30 000 cm^{-1} can be assigned unambiguously, applying a constant C/B ratio of ≈ 5.0, taken from the gaseous ion, in the d^5 Tanabe–Sugano matrices (*13*). The ligand-field parameters B(oct), B(tet), Δ(oct), and Δ(tet), obtained by this method from the optical spectra, are in good agreement with those of other transition metal ions in garnets (*14, 15*).

Mössbauer spectra as well as ligand-field spectra yield information on the chemical bonding of iron at the structural sites. An interesting question is the relationship between the isomer shift of ^{57}Fe and the Racah parameter B of Fe. Some correlated data based on the new assignment of the bands will be discussed.

Crystal Structure of Garnet

Garnets are of the general formula $c_3a_2d_3O_{12}$, where the symbols of the cations c(Ca, Mg, Mn^{2+}, Fe^{2+}, Y, Dy), a(Al, Cr, Ga, Ti, Fe^{3+}), and d(Si, Ti, Al, Ga, Fe^{3+}) refer to the point positions of the space group $1a3d$. The structure consists of a framework of three different coordination polyhedra around the cations c, a, and d: cO_8 triangular dodecahedra, aO_6 octahedra, and dO_4 tetrahedra (Fig. 1). For more detailed information about the crystal chemistry of garnets the reader is referred to review articles of Geller (*16*) and Novak and Gibbs (*17*).

Experimental

The garnets of our study, their chemical compositions, cell edges, colors, and origins are listed in Table II. The Mössbauer spectra were studied at constant acceleration in conjunction with a multichannel analyzer (1024 channels) using a source of ^{57}Co/Pd. The

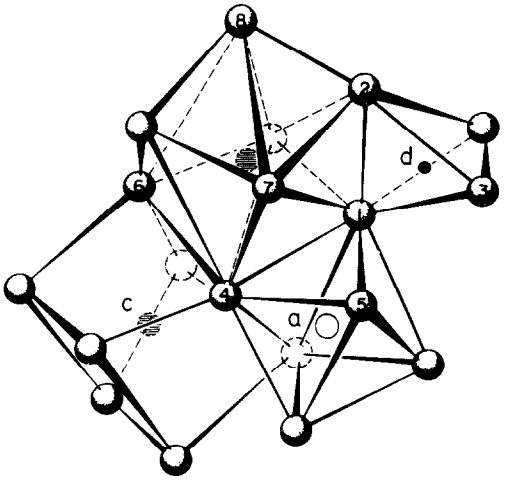

FIG. 1. Portion of the garnet structure after Novak and Gibbs (*17*).

absorber density was 5–7 mg Fe/cm^2. The velocity wave form was symmetric triangular. The two simultaneously obtained spectra were fitted independently assuming Lorentzian lines, and the average values of the two fits were taken as final values. More details are given in (*5*). The ligand-field spectra of our finely powdered samples were recorded between 8000 and 30 000 cm^{-1} by diffuse reflectance spectroscopy using a PMQ II spectrophotometer with infrasil optics. Carefully dried MgO was used as reference material. The low-temperature experiments were performed with a refrigerator cryostat in conjunction with a special remission sphere.

Results

The ligand-field spectra of the Ca garnets between 8000 and 28 000 cm^{-1} at 295 and 5°K are shown in Fig. 2a. The spectra exhibit several weak absorption bands; their resolution is improved at low temperatures. This can be observed, for example, in the two spectra of andradite $Ca_3Fe_2Si_3O_{12}$, where the absorption maximum at about 27 000 cm^{-1} is clearly visible at 5°K. For this reason the spectra of the Ca-free Y-bearing

TABLE II

CHEMICAL COMPOSITIONS, CELL EDGES, AND COLORS OF THE SAMPLES STUDIED

No.[a]	Garnet	Cell edge AE	Color
1a	$Y_3Fe_5O_{12}$	12.386	Olive-green
1b	$Y_3Fe_5O_{12}$	12.374	Olive-green
2	$Y_3Fe_{2.2}Ga_{2.8}O_{12}$	12.327	Greenish-yellow
3	$Y_3FeAl_4O_{12}$	12.095	Yellow
4	$Y_3FeGaAl_3O_{12}$	12.148	Grey-yellow
5	$YCa_2Fe_2Zr_2AlO_{12}$	12.618	Yellow-brown
6	$Ca_3Zr_2SiFe_2O_{12}$	12.610	Yellow-brown
7	$Ca_3Fe_2Si_3O_{12}$	12.061	Yellow
8	$(Mg, Fe)_3(Al, Fe)_2Si_3O_{12}$	11.533	Red-violet

[a] 1a, 2, 3, 4, 5: Moulin (*35*). 1b, Housley and Grant (*36*). 6, 7: Huggins *et al.* (*21*). 8: Natural andradite (topazolite) from Val Malenco, Italy; the precise formula is $Ca_{2.98}Fe_{1.95}Cr_{0.002}Ti_{0.002}Al_{0.04}Si_{3.02}O_{12}$ (Amthauer (*33*)). 9: Natural pyrope from Zöblitz, Saxony; the precise chemical formula is $Mg_{2.01}Ca_{0.36}Mn_{0.03}Fe^{2+}_{0.61}Al_{1.80}Cr_{0.10}Ti_{0.02}Fe^{3+}_{0.07}Si_{3.01}O_{12}$.

samples are presented in Fig. 2b only at 5°K. They show the same features as the Ca garnets with some minor shifts of the maxima. The observed positions of the bands and their assignment to the corresponding transitions in the energy-level scheme of a $3d^5$ ion in octahedral and tetrahedral coordination (cf. Fig. 3) are reported in Table III. The ligand-field energies were calculated by the energy equations of Fe^{3+} given in Tables IVa and b. The fit was done using the Tanabe–Sugano matrices on the basis of the following parameters:

$$B_0 \text{ (free ion)} = 930 \text{ cm}^{-1};$$

$$C_0/B_0 \cong 5.0; \Delta/B(\text{oct}) \cong 20;$$

$$\Delta/B(\text{tet}) \cong 12.$$

The B values were taken from the $^6A_1 \rightarrow {}^4_aE, {}^4A_1$, and ${}^4_bE$ transitions. The ligand-field parameter Δ of both positions was calculated from the ${}^4_aT_2$ band. The energy-level scheme in Fig. 3 was drawn using the experimental parameters Δ(oct), Δ(tet), B(oct), and B(tet). The choice of these parameters, based on the free ion spectra, as well as the fitting procedure of the experimental and calculated energies differs somewhat from the usual arguments and is discussed in a special paper (*18*).

Typical values for the isomer shifts and quadrupole splittings ΔE_Q of Fe^{3+} in garnets are listed in Table V. This table contains our own data as well as those of other investigators needed for the interpretation of the spectra. A typical spectrum of a garnet bearing Fe^{3+} at the octahedral and tetrahedral positions is shown in Fig. 4. Interpretation and assignment of this kind of spectrum are presented in detail in (*5*) and are in agreement with the studies in (*19–21*). The isomer shifts of the octahedral as well as of the tetrahedral Fe^{3+} reveal small but distinct variations within the different garnets. The quadrupole splittings are independent of the temperature but show interesting dependences on crystal chemical parameters.

TABLE III

OBSERVED ENERGIES OF THE ABSORPTION MAXIMA OF Fe^{3+} IN GARNETS

No.	Garnet	T (°K)	Absorption maxima (cm^{-1})								
1a, b	$Y_3Fe_5O_{12}$	5	10 800	14 700	16 200 16 700	19 800	20 700 21 300	22 500	—	—	—
1b		295	10 500	14 300	16 400	19 500	20 800 21 400	22 400	—	—	—
2	$Y_3Fe_{2.2}Ga_{2.8}O_{12}$	5	10 600	14 500	16 300	19 500	20 700 21 200	—	—	—	—
2		295	10 400	14 300	16 000	19 000	21 000	—	—	—	—
3	$Y_3FeAl_4O_{12}$	5	10 600	14 500	15 700 16 400	19 500	20 700 21 200	23 000	24 100	24 500	—
3		80	11 000	14 500	16 000 16 500	19 600	20 800 21 300	—	24 200	24 500	—
3		295	10 600	14 000	16 000	19 200	20 700 21 200	22 900	—	24 400	—
4	$Y_3FeGaAl_3O_{12}$	5	10 400	14 500	15 800 16 500	19 500	20 700 21 200	23 000	23 600	24 400	—
4		295	10 500	14 000	16 100	19 200	20 700 21 200	22 800	—	24 400	—
5	$YCa_2Zr_2Fe_2AlO_{12}$	5	11 300	14 700	16 600	19 400	20 700 21 000	22 700	24 100	24 400	
5		295	11 300	—	16 500	—	20 900	22 500	—	24 500	—
6	$Ca_3Zr_2Fe_2SiO_{12}$	5	11 200 11 200	14 800 14 800	16 300 16 700	19 500 19 700	21 000 21 100	22 500 22 700	24 100 24 200	24 500 24 700	— —
6		80			16 500 16 800						
7	$Ca_3Fe_2Si_3O_{12}$	5	11 700	15 500	—	—	—	22 700 23 000	—	—	26 200 27 000
7		295	11 600	—	—	—	—	22 700 23 000	—	—	—

Discussion

Interpretation of the Ligand-Field Spectra

The observed absorption bands in Figs. 2a and b of Fe^{3+} in the octahedral and tetrahedral sites of the garnet structure are due to electronic transitions from the ground state $^6A_1$ to the excited states $^4_aT_1$, $^4_aT_2$, $^4A_1$ ^4_aE, $^4_bT_2$, ^4_bE, and $^4_bT_1$ (cf. Fig. 3). these transitions are spin-forbidden and hence of relatively low intensity. It should be mentioned that the lack of inversion at the tetrahedral sites relaxes the parity rule and results in higher intensities of the tetrahedral absorption bands. Nevertheless, the assignment of the absorption maxima due to tetrahedral Fe^{3+} is more complicated, because no good samples bearing only tetrahedral Fe^{3+} are available, whose synthesis seems to be very difficult. Additionally the ligand absorption in the near uv is increased, if tetrahedral Fe^{3+} is present in the garnet. The assignment of the bands is based on the following arguments:

1. Assignment of the Δ-Independent Levels of Octahedral Fe^{3+}

The Mössbauer spectrum of andradite $Ca_3Fe_2Si_3O_{12}$ clearly shows that Fe^{3+} occupies mainly the octahedral positions. In agreement with this result the ligand-field spectrum can be assigned on the basis of octahedral Fe^{3+}. The main feature of the

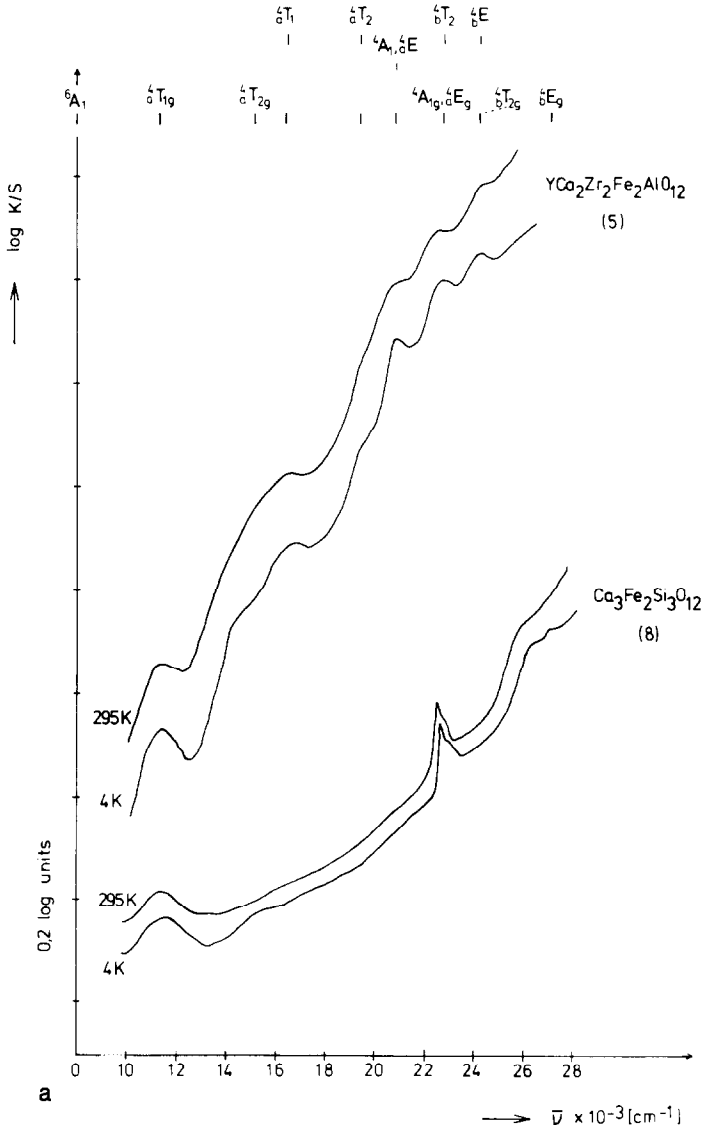

FIG. 2a. Ligand-field spectra of the Ca-bearing garnets at 5 and 295°K.

optical absorption spectrum is an intense and narrow peak at 22 700 cm^{-1} with a broader shoulder at the high-energy side. The small half-width and the splitting of about 250 cm^{-1} indicate that this absorption has to be assigned to a transition to the Δ-independent levels $^4A_{1g}$, $^4_aE_g$ (*22, 23*), whose energy degeneration is somewhat increased by second-order spin–orbit coupling and symmetry effects. The $^6A_{1g}$, $^4A_{1g}$, and $^4_aE_g$ levels have the same electronic configuration, i.e., $t_2^3e^2$, and transitions between these states are characterized by a very small half-width (*24*). The same behavior of the $^4A_{1g}$, $^4_aE_g$ levels is also often observed in Mn^{2+} compounds (*25, 26*), where the narrow line is assigned to the $^6A_{1g} \rightarrow {}^4_aE_g$, the broader to the $^6A_{1g} \rightarrow {}^4A_{1g}$ transition (*25, 26*).

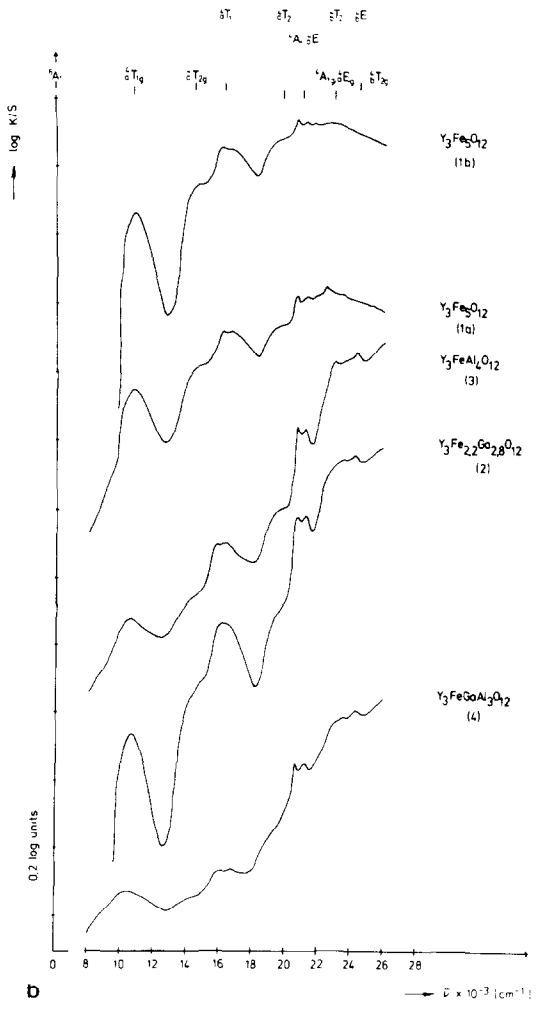

FIG. 2b. Ligand-field spectra of Y-bearing garnets at 5°K.

From the energy E of the $^4A_{1g}$, $^4_aE_g$ levels the interelectronic repulsion parameter of the octahedral Fe^{3+} B(oct) can be calculated using the equation of Tanabe and Sugano (*13*):

$$E(^4A_{1g}, {}^4_aE_g) = 10B + 5C = 35B.$$

Assuming $E = 22\,700\ \text{cm}^{-1}$ and $C/B = 5$, B(oct) is found to be $649\ \text{cm}^{-1}$. Knowing B(oct), one can calculate the energy of the second Δ-independent level $^4_bE_g$ according to the formula of (*13*):

$$E(^4_bE_g) = 17B + 5C = 42B.$$

With $C/B = 5$ an energy of $27\,258\ \text{cm}^{-1}$ is evaluated. An absorption band with a relatively small half-width is indeed observed at $27\,000\ \text{cm}^{-1}$ in the absorption spectrum of the andradite $Ca_3Fe_2Si_3O_{12}$ and can be assigned to the $^4_bE_g$ level. From this energy B is evaluated to be $643\ \text{cm}^{-1}$. Thus a value of $650 \pm 10\ \text{cm}^{-1}$ of B(oct) of Fe^{3+} in garnets seems to be reasonable. Single-crystal absorption spectra of the natural garnets spessartine $Mn_3(Al, Fe^{3+})_2Si_3O_{12}$, grossular $Ca_3(Al,Fe^{3+})_2Si_3O_{12}$, and pyrope $Mg_3(Al, Fe^{3+})_2Si_3O_{12}$ (*8, 9, 33*) confirm this

TABLE IV

OBSERVED AND CALCULATED ENERGIES OF THE ABSORPTION MAXIMA OF Fe^{3+} IN THE GARNETS STUDIED AT 5°K

Fe^{3+}(oct)					Fe^{3+}(tet)				
Garnet	E_{obs} (cm^{-1})	E_{cal}[a] (cm^{-1})	Term	Energy equation	Garnet	E_{obs} (cm^{-1})	E_{cal}[a] (cm^{-1})	Term	Energy equation
Y_3[b]	10 600 ± 200	10 050	$^4{}_aT_{1g}$	$-0.97\Delta + 8.3B + 6C$	Y_3	{16 000 ± 300; 16 350 ± 200}	15 670	$^4{}_aT_1$	$-0.93\Delta + 7.1B + 6C$
YCa_2[c]	11 300	10 350			YCa_2	16 600	15 670		
Ca_3[d]	11 700	11 020			Ca_3	—	—		
Y_3[b]	14 600 ± 100	14 635	$^4{}_aT_{2g}$	$-0.90\Delta + 13.7B + 6C$	Y_3	19 600 ± 200	19 480	$^4{}_aT_2$	$-0.77\Delta + 11.7B + 6C$
YCa_2[c]	14 700	14 905			YCa_2	19 400	19 480		
Ca_3[d]	15 500	15 535			Ca_3	—	—		
Y_3[b]	22 800	22 750	$^4A_{1g}, {}^4{}_aE_g$	$10B + 5C$	Y_3	{20 700 ± 100; 21 250 ± 100}	21 000	$^4A_1, {}^4{}_aE$	$10B + 5C$
YCa_2[c]	22 600	22 750			YCa_2	{20 700 ± 100; 21 000 ± 100}	21 000		
Ca_3[d]	{22 700; 23 000}	22 750			Ca_3	—	—		
Y_3[b]	24 400	24 620	$^4{}_bT_{2g}$	$-0.005\Delta + 13B + 5C$	Y_3	22 700	22 835	$^4{}_bT_2$	$-0.02\Delta + 13.3B + 5C$
YCa_2[c]	24 500	24 625			YCa_2	22 700	22 835		
Ca_3[d]	—	24 630			Ca_3	—	—		
Y_3[b]	—	27 300	$^4{}_bE_g$	$17B + 5C$	Y_3	—	25 200	$^4{}_bE_g$	$17B + 5C$
YCa_2[c]	—	27 300			YCa_2	—	25 200		
Ca_3[d]	27 000	27 300			Ca_3	—	—		

[a] Using $C_0/B_0 = 5.0$, $B_0 = 930\ cm^{-1}$ $(\Delta/B(oct)) = 20$ $(\Delta/B(tet)) = 12$; Y_3: $B(oct) = 650\ cm^{-1}$, $B(tet) = 600\ cm^{-1}$; $\Delta(oct) = 15\,300\ cm^{-1}$, $\Delta(tet) = 7200\ cm^{-1}$; YCa_2: $B(oct) = 650\ cm^{-1}$, $B(tet) = 600\ cm^{-1}$, $\Delta(oct) = 15\,000\ cm^{-1}$, $\Delta(tet) = 7200\ cm^{-1}$; Ca_3: $B(oct) = 650\ cm^{-1}$, $B(tet) = 600\ cm^{-1}$, $\Delta(oct) = 14\,300\ cm^{-1}$, $\Delta(tet) = 7200\ cm^{-1}$.

[b] Y_3, garnet samples 1–4.

[c] $YCa_2Zr_2Fe_2AlO_{12}$, sample 6.

[d] $Ca_3Fe_2Si_3O_{12}$, sample 7.

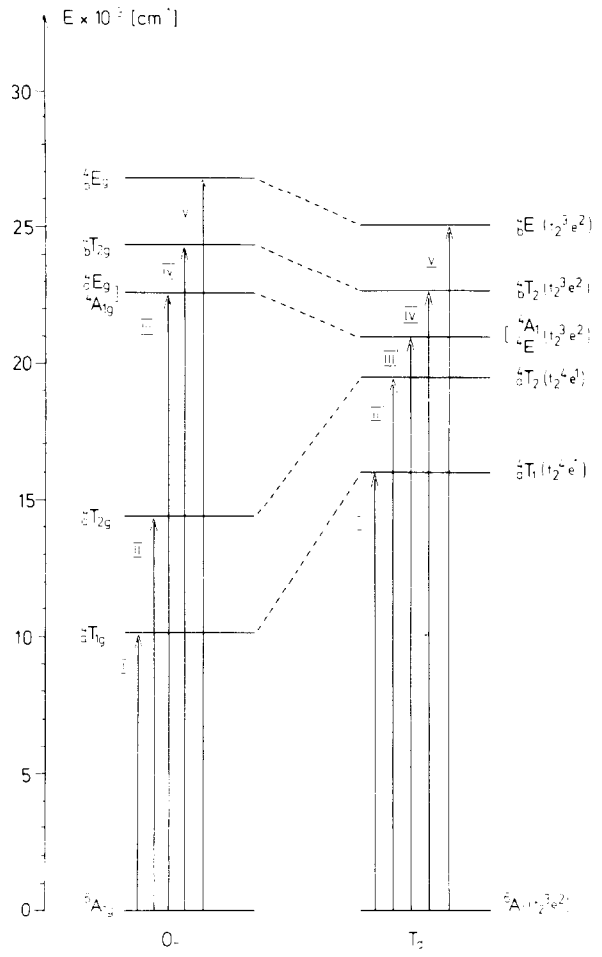

FIG. 3. Energy-level diagram of octahedral and tetrahedral Fe^{3+} in garnets.

assignment; they reveal the Δ-independent transitions to be at 22 700–23 300 cm^{-1} ($^4A_{1g}$, $^4_aE_g$) and at 27 000–27 200 cm^{-1} ($^4_bE_g$), from which a B(oct) value of 650 ± 10 cm^{-1} results. The experimental error of B(oct) depends mainly on the exact determination of the band maximum, which is found to be ±50 cm^{-1}. Additionally, the splitting of the $^4A_{1g}$, $^4_aE_g$ level is not considered, and frequently the average value of energy for these levels is used for the calculation of B.

The Fe-bearing Y garnets contain Fe^{3+} in both the octahedral and tetrahedral positions, as is obvious from the Mössbauer spectra (Fig. 4). For that reason the assignment of the ligand-field bands is more complicated. Because the interatomic distances and also the octahedral isomer shifts exhibit no abrupt change going from the Ca garnets to the Y garnets, only small shifts of the octahedral absorption maxima are expected. By analogy with the andradite spectrum (Fig. 2a) the band between 22 600 and 23 000 cm^{-1} in the Y -garnet spectra is likely to be the transition $^6A_{1g} \rightarrow {}^4A_{1g}$, $^4_aE_g$ of octahedral Fe^{3+}, which also yields a B value of 650 ± 10 cm^{-1}.

TABLE V

ISOMER SHIFTS δ AND QUADRUPOLE SPLITTINGS ΔE_Q OF Fe^{3+} IN DIFFERENT GARNETS AT ROOM TEMPERATURE

No.	Garnet	δ(o)[a] (mm/sec)	δ(t)[a] (mm/sec)	ΔE_Q(o)[b] (mm/sec)	ΔE_Q(t)[b] (mm/sec)	I(o)[c] (%)	I(t)[c] (%)	Ref.
8	$(Mg, Fe)_3(Al, Fe)_2Si_3O_{12}$	0.34	—	0.32	—	8.1	—	*[d]
8	$(Mn, Fe)_3(Al, Fe)_2Si_3O_{12}$	0.37	—	0.35	—	43.6	—	(5)
8	$Ca_3(Al, Fe)_2Si_3O_{12}$	0.39	—	0.58	—	21.2	—	(5)
7	$Ca_3Fe_2Si_3O_{12}$	0.41	—	0.56	—	100.0	—	*
7	$Y_3FeGaAl_3O_{12}$	0.39	0.10	0.38	0.95	61.5	38 5	*
2	$Y_3Fe_{2.2}Ga_{2.8}O_{12}$	0.39	0.12	0.39	0.93	59.8	40.2	*
3	$Y_3FeAl_4O_{12}$	0.41	0.10	0.35	0.97	55.0	45.0	(20)
3	$Y_3Fe_3Al_2O_{12}$	0.42	0.14	0.42	0.97	—	—	(20)
1	$Y_3Fe_5O_{12}$	0.39	0.16	0.48	1.02	—	—	(29)
5	$YCa_2Zr_2Fe_2AlO_{12}$	—	0.17	—	1.09	—	100.0	*
6	$Ca_3Zr_2Fe_2SiO_{12}$	—	0.18	—	1.05	—	100.0	*
6	$Ca_3Fe_2Ti_{1.42}Si_{1.58}O_{12}$	0.40	0.20	0.75	1.15	43.1	56.9	(5)
6	$NaCa_2Sb_2Fe_3O_{12}$	—	0.22	—	0.81	—	100.0	(34)
6	$Na_3Te_2Fe_3O_{12}$	—	0.23	—	0.51	—	100.0	(34)

[a] Referred to α-iron at room temperature.

[b] $\Delta E_Q = \frac{1}{2}eQV_{zz}[1+(\sqrt{/3})^2]^{1/2}$.

[c] Percentage of total absorption regarding corrections for different recoil free fractions according to (5).

[d] Asterisk denotes this work.

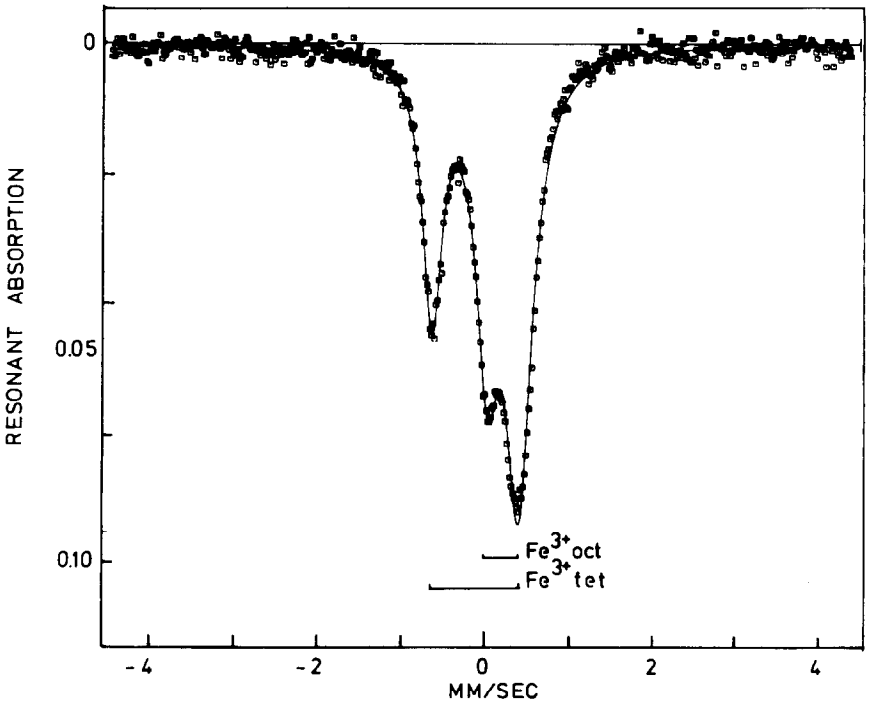

FIG. 4. Mössbauer spectra of ^{57}Fe in $Y_3Al_4FeO_{12}$ at 295°K.

2. Assignment of the ${}^4_aT_{1g}$ and ${}^4_aT_{2g}$ Levels of Octahedral Fe^{3+}

The assignment of the two lowest-energy absorption bands in the spectrum of andradite $Ca_3Fe^{3+}{}_2Si_3O_{12}$ is in agreement with most of the previous studies. The maxima at about 10 600 and 14 600 cm^{-1} in the spectra of the YFe garnets are due to the transitions ${}^6A_{1g} \rightarrow {}^4_aT_{1g}$ and $\rightarrow {}^4_aT_{2g}$ of octahedral Fe^{3+}. The ligand-field parameter Δ(oct) can be calculated from the ${}^4_aT_{2g}$ level at 14 600 cm^{-1} to be 15 300 cm^{-1} assuming B(oct) = 650 cm^{-1} (Table IIIa). The same transitions are measured at 11 300 and 15 000 (sh) cm^{-1} in the YCa garnets and at 11 600 and 15 500 (sh) cm^{-1} in andradite. According to the Tanabe–Sugano diagrams the energies of the two low-energy levels decrease with increasing ligand-field parameter Δ, e.g., decreasing octahedral cation–anion distance. Crystal structure refinements show that these distances are 1.937 Å in YAG, 1.995 Å in YGG, 2.019 Å in YIG (*27*), and 2.024 Å in andradite (*17*). According to these results and assuming that the ligand-field parameter Δ decreases with increasing cation–anion distance, the ${}^4_aT_{1g}$ and ${}^4_aT_{2g}$ levels would have the greatest energy in andradite. These two low-energy absorption bands of octahedral Fe^{3+} can also be observed even in the spectra of the garnets $Ca_3Zr_2SiFe_2O_{12}$ and $YCa_2Fe_2Zr_2AlO_{12}$, whose Mössbauer spectra reveal only the characteristic doublet of tetrahedral Fe^{3+}. This shows that the optical absorption spectra are very sensitive for small amounts of Fe^{3+} in a certain position of the garnet structure, although it should be mentioned that the Kubelka–Munk function reveals big differences at high values of reflectance.

3. Assignment of the ${}^4_bT_{2g}$ and ${}^4_bT_{1g}$ Levels of Octahedral Fe^{3+}

The ${}^6A_{1g} \rightarrow {}^4_bT_{2g}$ transition is calculated to have an energy of about 24 700 cm^{-1} assuming $C/B = 5$ and the energy equation of Table IV. The energy of this level is also nearly independent of the ligand-field strength, and the ${}^4_bT_{2g}$ level has the same electronic configuration as the ground state, i.e., $t_{2g}^3e_g^2$. This should again result in a small half-width of the corresponding absorption band. At energies between 24 000 and 25 000 cm^{-1} an absorption maximum is observed at about 24 500 cm^{-1}, which is assigned to the ${}^4_bT_{2g}$ level. The ${}^6A_{1g_1} \rightarrow {}^4_bT_{1g}$ transition is calculated to have an energy of more than 30 000 cm^{-1}. An absorption band corresponding to that transition could not be resolved in our spectra because of the strongly increasing ligand absorption in the near UV.

4. Assignment of the Δ-Independent Levels of Tetrahedral Fe^{3+}

The narrow and intense band, which in most of our samples is also split into two maxima at about 20 700 and 21 300 cm^{-1}, should be interpreted as the transition to the first Δ-independent level ${}^4A_1$, ${}^4_aE$ of tetrahedral Fe^{3+}. The splitting must be somewhat greater than the octahedral one of 250 cm^{-1} and can be due to two effects: (i) Lohr (*26*) has pointed out that the influence of covalency may lift the degeneracy of the two levels ${}^4A_1$ and ${}^4_aE$; (ii) the considerable distortion of the tetrahedron causes an additional splitting of the tetrahedral levels. In garnets, the distortion of the tetrahedron is greater than that of the octahedron. As shown by structure refinements, the bond angle opposite the shared edge of the tetrahedron (ideally 109°25′) varies between 98 96° in YIG (*27*) and 102.64° in andradite $Ca_3Fe_2Si_3O_{12}$ (*17*), whereas the octahedral bond angle (ideally 90.00°) opposite the shared edge varies between 83.62° in YIG (*27*) and 91.12° in andradite (*17*). This difference in distortion is also reflected by the quadrupole splitting of ^{57}Fe, which is twice as large for tetrahedral as for octahedral Fe^{3+} (cf. Table IV). Because of this large splitting the evaluation of B(tet) is very problematic.

Assuming an average energy of 21 000 cm^{-1}, B(tet) is calculated to be 600 cm^{-1}, i.e., lower than B(oct). In agreement with this result the isomer shift of tetrahedral Fe^{3+} is lower than the octahedral one (cf. Table V). This will be discussed in more detail in the next section. With B(tet) = 600 cm^{-1} the second Δ-independent level ${}^4_bE_g$ is calculated to have an energy of 25 200 cm^{-1}, but no absorption band can be observed at that energy, because of the poor resolution of the spectra at these energies.

In the case of octahedral Fe^{3+} we have evaluated B(oct) from the sharp peak at 22 700 cm^{-1}, i.e., the ${}^4_aE_g$ level (*25, 26*), and not from the average energy of both levels. If we calculate B(tet) from the first of the two levels at 20 700 cm^{-1}, we get a value of about 590 cm^{-1} for B(tet). This results in an energy of 24 780 cm^{-1} for the ${}^4_bE$ level, which may be assigned to the maximum at about 24 500 cm^{-1}, assuming a small shift to lower energies. If we calculate B(tet) from the second of the two ${}^4A_1$, ${}^4_aE$ levels at about 21 300 cm^{-1}, we get a value of 610 cm^{-1} for B(tet) and a value of 25 620 cm^{-1} for the ${}^4_bE$ level. A small band is observed at 26 200 cm^{-1} in the absorption spectrum of andradite $Ca_3Fe_2Si_3O_{12}$. This could be the transition ${}^6A_1 \rightarrow {}^4_bE$ of tetrahedral Fe^{3+}. But this assignment requires an unreasonably large difference between the calculated and observed energies of the ${}^4_bE$ level. Regarding the great variations of the tetrahedral isomer shift a change of B(tet) can be expected, resulting in a shift of the absorption bands. Unfortunately, the first independent level cannot be observed in our silicate garnet sample.

Thus, the evaluation of B(tet) has a very large error and the high-energy levels of tetrahedral Fe^{3+} cannot be assigned unambiguously. From our present data the "average" value of B(tet), 600 cm^{-1}, seems to be the most reasonable.

5. Assignments of the ${}^4_aT_1$ and ${}^4_aT_2$ Levels of Tetrahedral Fe^{3+}

The two low-energy transitions ${}^6A_1 \rightarrow {}^4_aT_1$ and ${}^6A_1 \rightarrow {}^4_aT_2$ are found at about 16 200 and 19 600 cm^{-1} in the Y garnets. Δ(tet) was calculated from the ${}^4_aT_2$ level to be 7200 cm^{-1}. The band at 16 200 cm^{-1} is distinctly split in most cases by 600–800 cm^{-1} (Fig. 2b), as a result of the large tetrahedral site distortion discussed above.

6. Assignment of the ${}^4_bT_2$ Level of Tetrahedral Fe^{3+}

The assignment of the ${}^4_bT_2$ level is as uncertain as that of the second Δ-independent level ${}^4_bE$. Assuming B(tet) = 600 cm^{-1}, an energy of about 22 800 cm^{-1} is calculated for the ${}^2_bT_2$ level. If B(tet) = 610 cm^{-1}, ${}^4_bT_2$ has an energy of 23 219 cm^{-1}. The corresponding absorption bands would be hidden by the intense transition ${}^6A_{1g} \rightarrow {}^4A_{1g}$, ${}^4_aE_g$ of octahedral Fe^{3+}.

7. Comparison of the Ligand-Field Parameters of Different Transition Metal Ions in Garnets

The ligand-field parameters Δ(oct), Δ(tet), and B(oct) of the Fe^{3+} ion should be comparable with those of other transition metal ions such as V^{3+} and Cr^{3+} in an oxygen coordination. In Table VI the ligand-field parameters of these transition metal ions in garnets are listed, and they show that the ligand-field parameters of the Fe^{3+} are in good agreement with the values of the other ions. This confirms that our band assignment of the optical spectra of the Fe^{3+}-bearing spectra is reasonable. The ratio of the tetrahedral to the octahedral ligand-field parameter is 0.47, which differs somewhat from the ideal value of 0.44, assuming in this case the same distances for the Fe–O bonds in the octahedron and the tetrahedron.

TABLE VI

LIGAND-FIELD STRENGTH Δ AND RACAH PARAMETERS B(oct) AND B(tet) OF V^{3+}, Cr^{3+}, AND Fe^{3+} IN GARNETS

Ion	Garnet	Δ(o)	Δ(t)	r[a]	B(o)	B(t)	β(o)[b]	β(t)[b]	Ref.[c]
V^{3+}	$Y_3Al_5O_{12}$	17 000	8500	0.5	600	—	0.67	—	(*14*)
Cr^{3+}	$Y_3Cr_2Al_3O_{12}$	16 400	—	—	600	—	0.65	—	(*15*)
Cr^{3+}	$Y_3Cr_2Ga_3O_{12}$	16 150	—	—	625	—	0.68	—	(*15*)
Cr^{3+}	$Ca_3Cr_2Si_3O_{12}$[d]	16 260	—	—	645	—	0.70	—	(*33*)
Cr^{3+}	$Mg_3(Al, Cr)_2Si_3O_{12}$[e]	17 570	—	—	652	—	0.71	—	(*33*)
Fe^{3+}	$Y_3Fe_5O_{12}$	15 200	7200	0.47	650	600	0.70	0.65	*
Fe^{3+}	$Ca_3Fe_2Si_3O_{12}$	14 300	—	—	650	—	0.70	—	*

[a] $r = \Delta(\text{oct})/\Delta(\text{tet})$.
[b] $\beta = B(\text{complex})/B(\text{gaseous ion})$.
[c] Asterisk denotes this work.
[d] Idealized formula of the natural mineral uvarowite.
[e] Idealized formula of the natural mineral pyrope.

Racah Parameters B and Isomer Shifts of Fe^{3+} in Garnets

In most of the previous investigations B(oct) of Fe^{3+} is found to be smaller than B(tet) of Fe^{3+} in oxide garnets (cf. Table I), whereas the evaluation of our data leads to the conclusion that B(oct) is larger than B(tet) (cf. Table IVa, b) in agreement with the behavior of other transition metal ions in oxides. For example, Reinen (*30*) reported B(tet) of Ni^{2+} in the tetrahedral sites of ZnO to be 805 cm^{-1}, whereas B(oct) of Ni^{2+} in the octahedral positions of MgO is found to be 865 cm^{-1}. According to Jørgenson (*28*), B decreases with increasing radial expansion of the d-electron functions of the cation, caused, at least in part, by cation–anion orbital overlap. This overlap is expected to be stronger in the tetrahedron because of the smaller tetrahedral cation–anion distance in oxide garnets. This distance is 1.866 Å in YIG (*27*), whereas the octahedral distance is 2.019 Å in andradite (*17*). According to this model B(tet) should be smaller than B(oct).

One of the most important Mössbauer parameters for the discussion of chemical bonding is the isomer shift δ, which is about twice as large for the octahedral as for the tetrahedral Fe^{3+} (Table V). These differences are well understood on the basis of different coordination numbers and usually different cation–anion distances resulting in an increased s-electron density at the tetrahedral positions.

Correlating ligand-field and Mössbauer parameters, one can conclude the following. The isomer shift δ depends mainly on variations of the s-electron density at the nucleus, whereas B reflects changes of the d-electron functions. In the MO-bonding model the s electrons, especially 4s, form σ bonds with one of the ligand p orbitals, which are strongly influenced by cation–anion distances. Thus, the isomer shift is very sensitive to variations in the σ bonding. Nevertheless, a radial expansion of the 3d orbitals causes a diminished shielding effect of the d electrons and thus an increase of the s electron density at the nucleus. Thus, a decrease of B is in agreement with a decrease of the isomer shift. The smaller B(tet) and δ(tet) values with respect to the octahedral values are also in good agreement with these considerations.

Also within the different garnets, the isomer shifts of iron in both positions show

small but distinct differences. The increase of the isomer shift (decrease of the electron charge density at the nucleus) of the octahedral Fe^{3+} from pyrope $Mg_3(Al, Fe^{3+})_2Si_3O_{12}$ ($\delta = 0.34$ mm/sec) to the Y and Ca garnets ($\delta = 0.40$–0.41 mm/sec) can be explained by the increasing iron–oxygen distance a–O (pyrope a–O = 1.886 Å, andradite a–O = 2.024 Å (*17*)), resulting in a decrease of the s-electron density at the iron nucleus.

The same effect can be observed for the tetrahedral isomer shift. For example, within the YAG–YIG solid solutions the increase of the tetrahedral cation–anion distance d–O is found to be 1.761 Å in YAG and 1.866 Å in YIG, δ(tet) is determined to be 0.10 mm/sec in $Y_3Al_4FeO_{12}$ and 0.17 mm/sec in $Y_3Fe_5O_{12}$ (*29*). The cation substitution AlFe leads to an expansion of the garnet structure, which causes a decrease of the bonding orbital overlap and thus the electron density at the nucleus. On the other hand the differences between the tetrahedral isomer shifts δ(tet) of the Y and Ca garnets cannot be explained by geometrical considerations alone, because the d–O distances of the Ca garnets (d–O = 1.645–1.643 Å (*17*)) are smaller than those of the Y garnets (d–O = 1.761–1.866 Å (*27*)), whereas the shifts are greater. This increase can possibly be explained by contrapolarization effects (*30, 31*), which are also confirmed by increasing Δ values from andradite $Ca_3Fe_2Si_3O_{12}$ ($\Delta = 14\,300$ cm^{-1}) to $Y_3(Fe^{3+}, Me^{3+})_5O_{12}$ ($\Delta = 15\,200 \pm 100$ cm^{-1}). Tetrahedra and octahedra share corners in the garnet structure. The substitution of a trivalent cation (Fe, Al) by a tetravalent cation (Zr, Ti) or a hexavalent cation (Te) in the octahedral sites is accompanied by a decrease of the s-electron density at the Fe nucleus at the tetrahedral site. Thus δ(tet) is found to be 0.10–0.16 mm/sec in Y(Al)G, 0.19 mm/sec in $Ca_3Zr_2Fe_2SiO_{12}$ and 0.23 mm/sec in $Na_3Te_2Fe_3O_{12}$. It should also be noted, that the magnetic hyperfine fields at the d sites show similar variations.

The systematic variations of δ(oct) as well as δ(tet) within the different garnets cannot be detected in the case of B(oct) and B(tet) evaluated from our remission spectra. Variations, if any, may be observed in the case of B(tet), as is indicated by the great differences of δ(tet), for example, between the Y garnets and the silicate garnets. But the tetrahedral bands are not well resolved in our andradite spectrum. Manning reports a decrease of B(oct) from andradite $Ca_3Fe_2Si_3O_{12}$ (B(oct) = 593 cm^{-1} (*7*)) to spessartine $Mn_3(Al, Fe^{3+})_2Si_3O_{12}$ (B(oct) = 500 cm^{-1} (*7*)), using the energy difference $\Delta E = 7B$ of the two Δ-independent levels, but his calculation of B(oct) requires changing C/B ratios (5.65 in spessartine and 7.35 in andradite). This implies that the ligand oxygen has different influence on the interelectronic repulsion parameters B and C. On the other hand B_0 and C_0 of the free ion should be decreased in a complex in the same way, resulting in constant C/B ratios (*18*).

Finally, it should be mentioned that the octahedral and tetrahedral quadrupole splittings ΔE_Q also reveal distinct variations, which are not always in agreement with the geometrical site distortions as determined from X-ray diffraction crystal structure refinements, but are strongly influenced by overlap distortion effects as in the case of silicate garnets (*32*).

Acknowledgments

We thank Dr. D. Reinen, Fachbereich Chemie der Universität Marburg, and Dr. S. S. Hafner, Institut für Mineralogie der Universität Marburg, for many useful discussions, and Miss V. Gerlich for technical assistance.

References

1. W. V. NICHOLSON AND G. BURNS, *Phys. Rev.* **133**, 1568 (1964).

2. J. J. VAN LOEF, *Physica* **22**, 2102 (1966).
3. G. A. SAWATZKY, F. VAN DER WOUDE, AND A. H. MORRISH, *Phys. Rev.* **183**, 383 (1969).
4. I. S. LYUBUTIN AND L. G. LYUBUTINA, *Sov. Phys.–Cryst.* **15**, 708 (1971).
5. G. AMTHAUER, H. ANNERSTEN, AND S. S. HAFNER, *Z. Kristallogr.* **143**, 14 (1976).
6. D. L. WOOD AND J. P. REMEIKA, *J. Appl. Phys.* **38**, 1038 (1967).
7. P. G. MANNING, *Canad. Mineral.* **10**, 677 (1970).
8. P. G. MANNING, *Canad. Mineral.* **12**, 826 (1972).
9. R. K. MOORE AND W. B. WHITE, *Canad. Mineral.* **12**, 791 (1972).
10. Y. SUGITANI, K. TAGAWA, AND K. KATO, *Mineral. J.* **7**, 445 (1974).
11. G. B. SCOTT, D. E. LACKLISON, AND I. L. PAGE, *Phys. Rev. B* **10**, 971 (1974).
12. T. K. VIEN, I. L. DORMANN, AND H. LE GALL, *Phys. Status solidi.* **71**, 731 (1975).
13. Y. TANABE AND S. SUGANO, *J. Phys. Soc. (Japan)* **9**, 753 (1954).
14. M. J. WEBER AND L. A. RISEBERG, *J. Chem. Phys.* **55**, 2032 (1971).
15. D. REINEN, *Struct. Bond.* **6**, 30 (1969).
16. S. GELLER, *Z. Kristallogr.* **125**, 1 (1967).
17. G. A. NOVAK AND G. V. GIBBS, *Amer. Mineral.* **56**, 791 (1971).
18. P. KÖHLER AND D. REINEN, private communication, 1978.
19. E. R. CZERLINSKY, *Phys. Status solidi.* **34**, 483 (1969).
20. E. R. CZERLINSKY AND R. A. MACMILLAN, *Phys. Status solidi.* **41**, 333 (1970).
21. F. E. HUGGINS, D. VIRGO, AND H. G. HUCKENHOLZ, *Amer. Mineral.* **62**, 475 (1977).
22. S. V. GRUM-GRZHIMAILO, N. A. BRILLIANTOV, D. T. SVIRIDOV, AND R. K. SVIRIDOVA, *Opt. Spectrosk. (USSR)* **14**, 118 (1963).
23. P. G. MANNING, *Earth Sci.* **4**, 1039 (1970).
24. L. E. ORGEL, *J. Chem. Phys.* **23**, 1004 (1955).
25. S. KOIDE, *Philos. Mag.* **3**, 607 (1958).
26. L. L. LOHR, *J. Chem. Phys.* **55**, 27 (1971).
27. F. EULER AND J. BRUCE, *Acta Crystallogr.* **19**, 971 (1965).
28. C. K. JØRGENSEN, "Orbitals in Atoms and Molecules," Academic Press, London (1962).
29. G. N. BELOZERSKII, Y. P. KHIMICH, AND V. N. GITROVICH, *Phys. Status solidi.* **79**, K 125 (1977).
30. D. REINEN, *Ber. Bunsenges. Phys. Chem.* **69**, 82 (1964).
31. J. FERGUSON, *J. Chem. Phys.* **39**, 890 (1963).
32. S. S. HAFNER, M. RAYMOND, D. VIRGO, AND F. E. HUGGINS, *Carnegie Inst. Wash. Yearbook* **75**, 739 (1976).
33. G. AMTHAUER, *N. Jb. Miner. Abh.* **126**, 158 (1976).
34. A. P. DODOKIN, I. S. LYUBUTIN, B. V. MILL, AND V. P. PERKOV, *Sov. Phys. JETP* **36**, 526 (1973).
35. N. MOULIN, Dissertation, Bonn (1969).
36. R. M. HOUSLEY AND R. W. GRANT, *Phys. Rev. Lett.* **29**, 203 (1972).